Journal of Sound and Vibration (1997) **199**(2), 285–297

A COMPARATIVE STUDY OF VIBRATING LOADED PLATES BETWEEN THE RAYLEIGH-RITZ AND EXPERIMENTAL METHODS

K. H. Low, G. B. Chai and G. S. Tan

School of Mechanical and Production Engineering, Nanyang Technological University, Nanyang Avenue, Singapore 639798, *Republic of Singapore*

(*Received* 26 *July* 1995, *and in final form* 29 *May* 1996)

Natural frequencies of rectangular plates carrying a concentrated mass are obtained by employing a set of trigonometric beam functions in the Rayleigh-Ritz method. Two models of the energy method using one-term and 100-term model are used in the study. Results obtained from the analytical study using the energy method are compared with those measured experimentally. It is found that the 100-term analytical model can generally predict well the experimental frequencies of a plate carrying an arbitrarily placed concentrated mass, whereas the one-term analytical model is only good for estimating the first-mode frequency of a plate carrying a centrally placed mass.

1. INTRODUCTION

Electronic systems in aircraft or aerospace applications are usually housed in electronic enclosures with a chassis. To ensure equipment reliability, it is of vital importance that they are designed to withstand dynamic stresses. There is no simple and accurate rule involving the chassis weight and size that allows the designer to predict the natural frequencies and mode shapes of the loaded chassis. Hence the natural frequencies of lateral vibrations of a rectangular plate carrying a concentrated mass are often of interest [1–8]. Rectangular plates do not have an exact solution unless at least two opposite edges are simply supported [9]. Natural frequencies of plates involving other edge conditions are estimated by the Rayleigh-Ritz method using shape functions satisfying edge conditions in both directions. Beam characteristic functions were used in the Rayleigh-Ritz method to obtain frequency estimates for the plates with various edge conditions by Leissa [9]. A study by Bhat [10] used boundary characteristic orthogonal polynomials in the energy method. His later work [11] introduced a reduction method by assuming a deflection shape in one direction consistent with the boundary conditions and applying Galerkin's averaging technique and the Kantorovich method to obtain frequency coefficients. In another work [4], the fundamental frequency of vibrating beams and plates carrying finite masses was determined by using the optimized Rayleigh method, with account taken of the effects of both their translational and rotational inertias. Chai [7, 8] presented a frequency analysis for the loaded plates by double trigonometric series.

In the present study, the frequencies of rectangular plates carrying a concentrated mass have been evaluated by using a set of combined trigonometric function in the Rayleigh-Ritz method. Numerical results are compared with those obtained using a shaker experimental set-up.

0022–460X/97/020285 + 13 $25.00/0/sv960633

TABLE 1

Assumed shape functions using trigonometric functions

Two opposite ends	$X_m(x)$	$Y_n(y)$	m	n
S-S	$\sin(m\pi x/a)$	$\sin(n\pi y/b)$	1, 2, 3, . . .	1, 2, 3, . . .
C-C	$\sin(\pi x/a)\sin(m\pi x/a)$	$\sin(\pi y/b)\sin(n\pi y/b)$	1, 2, 3, . . .	1, 2, 3, . . .
C-S	$\sin(\pi x/2a)\sin(m\pi x/2a)$	$\sin(\pi y/2b)\sin(n\pi y/2b)$	2, 4, 6, . . .	2, 4, 6, . . .

2. MODELS STUDIED

2.1. ENERGY METHOD

The Rayleigh-Ritz is an energy method (EM) used in the present formulation and a multiple-term trigonometric function is used to represent the appropriate mode shape.

Consider a thin plate carrying a concentrated mass M at position $x = k$ and $y = h$ with the axes origin at one of the corners of the plate, the strain energy of bending for the case of free vibration is [12, 13]

$$U_{max} = \frac{D}{2}\int_0^a\int_0^b \left\{\left(\frac{\partial^2 w}{\partial x^2}+\frac{\partial^2 w}{\partial y^2}\right)^2 - 2(1-\nu)\left[\frac{\partial^2 w}{\partial x^2}\frac{\partial^2 w}{\partial y^2} - \left(\frac{\partial^2 w}{\partial x\,\partial y}\right)^2\right]\right\} \mathrm{d}x\,\mathrm{d}y, \tag{1}$$

where $D = Et^3/[12(1-\nu^2)]$ is the flexural rigidity of the plate, E is Young's modulus, ν is the Poisson ratio, and t is the thickness of the plate.

The maximum kinetic energy of the plate carrying a concentrated mass (excluding the rotary inertia effect) is given as

$$T_{max} = \frac{\omega^2}{2}\left\{\int_0^b\int_0^a \gamma(x, y)w^2(x, y)\,\mathrm{d}x\,\mathrm{d}y + M(k, h)w^2(k, h)\right\}, \tag{2}$$

where $\gamma(x, y)$ is the mass of the plate per unit area, $M(k, h)$ is the concentrated mass at co-ordinates $\langle k, h\rangle$, $w(x, y)$ is the assumed deformed shape, and ω is the frequency of the plate. For the system to be conservative the maximum bending energy equals the maximum kinetic energy, hence resulting in the well-known Rayleigh's quotient:

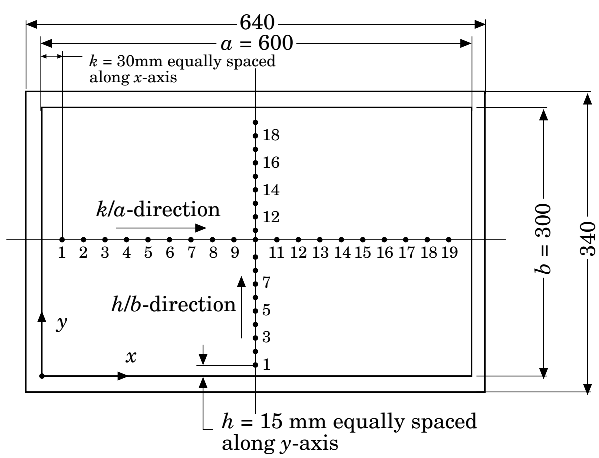

Figure 1. Location of grid points for the 600 × 300 mm plate.

TABLE 2

Configurations of the loaded plate system

Aluminium plate		
Size (mm)	mass (kg)	Concentrated mass (kg)
$600 \times 300 \times 2$	1·151	0·096
$500 \times 500 \times 2$	1·594	0·301
$500 \times 200 \times 2$	0·691	

$$\omega^2 = U_{max}/T^*, \tag{3}$$

where

$$T^* = \tfrac{1}{2}\int_0^b \int_0^a \gamma(x, y) w^2(x, y)\, \mathrm{d}x\, \mathrm{d}y + \tfrac{1}{2} M(k, h) w^2(k, h).$$

The Rayleigh-Ritz method is an extension of Rayleigh's method which not only provides a means of determining a more accurate value of the fundamental frequency, but also gives an approximation of the higher frequencies and mode shapes. Mathematically a shape function in the form of a series is written as [14]

$$w(x, y) = \sum_{m=1}^{M} \sum_{n=1}^{N} A_{mn} X_m(x) Y_n(y), \tag{4}$$

where $X_m(x)$ and $Y_n(y)$ are appropriate shape functions that satisfy at least the geometrical boundary conditions of the plate, and A_{mn} are the unknown coefficients of the functions. Substitution of the assumed function (4) into the total vibrating energy of equations (1) and (2) yields

$$U_{max} = \tfrac{1}{2} \sum_m \sum_n \sum_p \sum_q K_{mnpq} A_{mn} A_{pq}, \quad T^* = \tfrac{1}{2} \sum_m \sum_n \sum_p \sum_q S_{mnpq} A_{mn} A_{pq}, \tag{5, 6}$$

where

$$K_{mnpq} = \int\!\!\int \{(X''_m Y_n + X_m \ddot{Y}_n)(X''_p Y_q + X_p \ddot{Y}_q) + 2(1 - \nu)(X_m X''_p Y_n \ddot{Y}_q$$
$$- X'_m X'_p \dot{Y}_n \dot{Y}_q)\}\, \mathrm{d}x\, \mathrm{d}y, \tag{7}$$

$$S_{mnpq} = \gamma \int\!\!\int (X_m X_p Y_n Y_q)\, \mathrm{d}x\, \mathrm{d}y + M X_m(k) X_p(k) Y_n(h) Y_q(h). \tag{8}$$

In equations (7) and (8), prime denotes differentiation with respect to x and dot denotes differentiation with respect to y.

The minimization of equation (3) with respect to each of the coefficients yields

$$\partial U_{max}/\partial A_{mn} - (U_{max}/T^*)(\partial T^*/\partial A_{mn}) = 0. \tag{9}$$

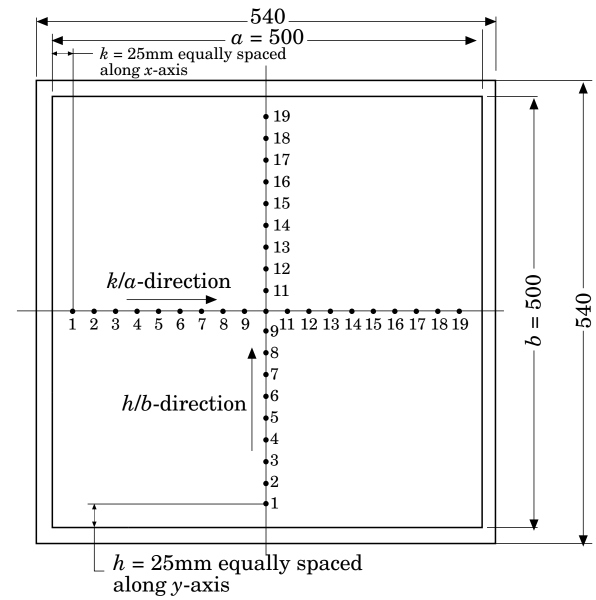

Figure 2. Location of grid points for the 500 × 500 mm plate.

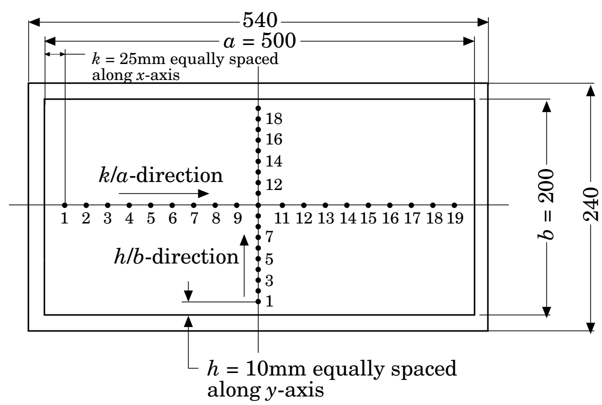

Figure 3. Location of grid points for the 500 × 200 mm plate.

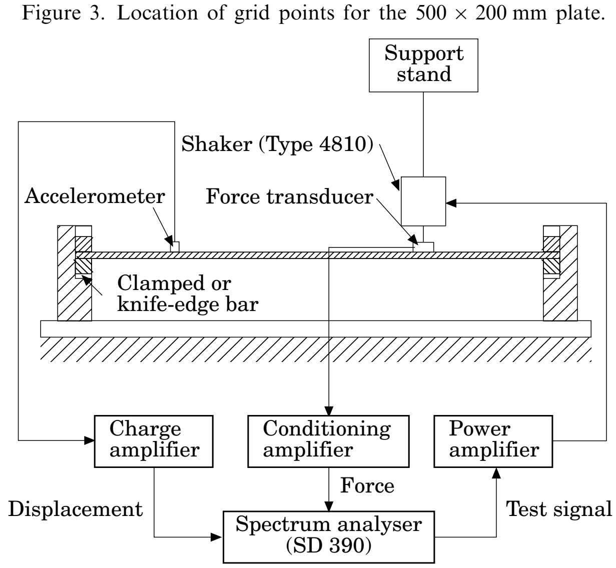

Figure 4. Schematic layout of the experimental set-up.

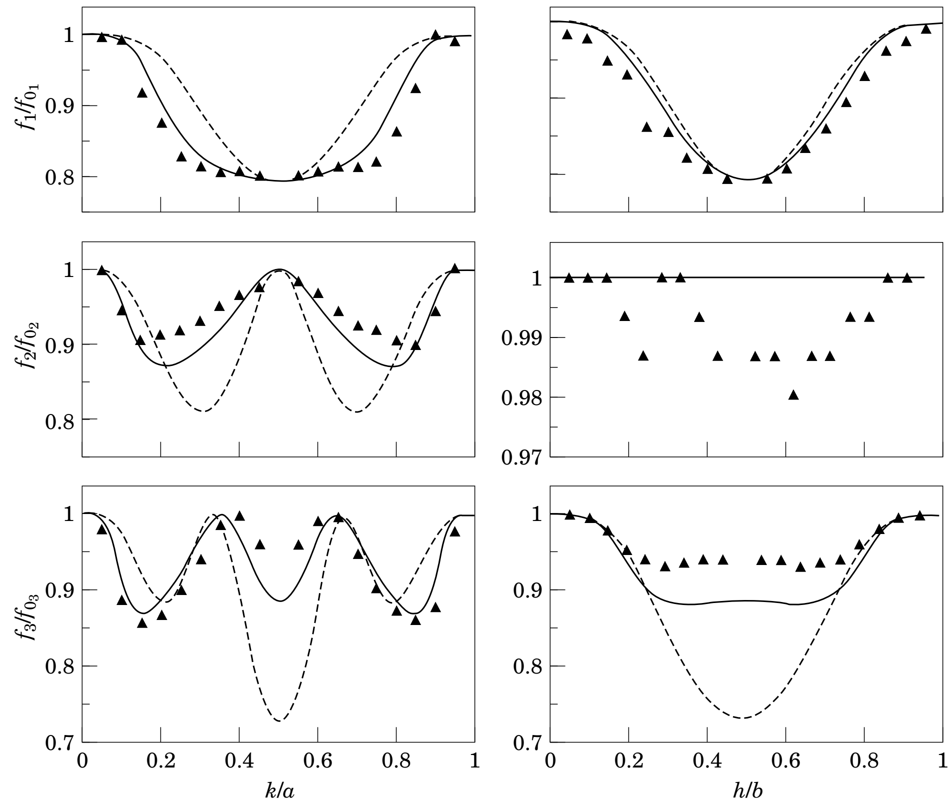

Figure 5. Comparative results of the 600 × 300 mm CCCC plate carrying a mass of 0.096 kg. ▲, experimental; – – – – –, EM one-term; ——, EM 100-term.

Since $\omega^2 = U_{max}/T^*$, the above equation can be written as:

$$\partial U_{max}/\partial A_{mn} - \omega^2(\partial T^*/\partial A_{mn}) = 0. \tag{10}$$

The above equation can be rearranged in a compact matrix format:

$$D[\mathbf{K}]\{\mathbf{A}\} = \omega^2[\mathbf{S}]\{\mathbf{A}\}, \tag{11}$$

where $[\mathbf{K}]$ is the stiffness matrix with its coefficients being defined in equation (7), $[\mathbf{S}]$ is the mass matrix with its coefficients being defined in equation (8) and $\{\mathbf{A}\}$ is the vector of the unknown coefficients.

Specifying the required number of M terms and N terms in the postulated modal shape function of equation (4), the minimization process yields a set of $M \times N$ linear homogeneous simultaneous equation (10) and thus equation (11) will give $M \times N$ stiffness and mass matrices. A standard numerical eigensolution scheme written in a computer language by Linfield and Penny [15] was used to extract the eigenvalues and their corresponding eigenvectors for the plate's natural frequencies and the corresponding mode shapes.

As reflected in equations (2) and (4), the accuracy of the Rayleigh method depends on the selection of compatible shape functions, $X_m(x)$ and $Y_n(y)$. A set of beam functions shown in Table 1 is used in the present study; the origin of the x-y axes is at one corner of the plate as shown in Figure 1. The letters S and C mean simply supported and clamped respectively. By combining the beam functions given in Table 1 to satisfy the various plate boundary conditions, a total of 6 distinct cases can be obtained: SSSS, SSSC, CCCC, CSCS, CCSS and CCCS. However, only 2 distinct cases will be emphasized in this study, CCCC and CSCS (and SCSC). In the present study, two sets of the solution using the functions for S-S and C-C of Table 1 are generated, namely, EM one-term ($m = n = 1$) and EM 100-term ($m = n = 10$). It was found in references [7, 8] that the 100 terms in the series expansion is necessary for convergence; in particular for cases of off-centre loaded mass.

2.2. EXPERIMENTS

Modal testing was conducted to investigate the effect on the system frequencies of a concentrated mass located at various plate locations. The testing configurations of the loaded plate system are shown in Table 2. A shaker system (see Figure 4) was set up to obtain a set of frequencies of the loaded plate as the concentrated mass is shifted from one position to another. These positions were marked by grid points equally spaced along the plate's centre-lines in both the x- and y-directions, as shown in Figures 1–3. For example, position 10 is the plate's centre ($k/a = 0{\cdot}5$, $h/b = 0{\cdot}5$) of both the x- and y-axes.

During the experimental process, the rectangular plate is supported by either/both the knife-edge and the square bars depending on the types of boundary conditions to be tested. The shaker is suspended from the support stand. As seen in Figure 4, the spectrum analyser sends a known signal to activate the shaker through the power amplifier. The shaker then vibrates the plate within a range of specified frequencies and the responses are picked up by the accelerometer and the force transducer via the charge amplifier and the conditioning

TABLE 3

Experimental results of the 600 × 300 *mm CCCC plate carrying a mass of* 0·096 kg

Position	k/a	f_1/f_{0_1}	f_2/f_{0_2}	f_3/f_{0_3}	h/b	f_1/f_{0_1}	f_2/f_{0_2}	f_3/f_{0_3}
1	0·05	0·994	1·000	0·979	0·05	0·985	1·000	1·000
2	0·10	0·993	0·944	0·888	0·10	0·978	1·000	0·997
3	0·15	0·917	0·906	0·858	0·15	0·951	1·000	0·980
4	0·20	0·875	0·913	0·868	0·20	0·931	0·993	0·953
5	0·25	0·828	0·919	0·902	0·25	0·862	0·987	0·941
6	0·30	0·813	0·931	0·941	0·30	0·856	1·000	0·932
7	0·35	0·806	0·951	0·986	0·35	0·822	1·000	0·936
8	0·40	0·806	0·965	1·000	0·40	0·807	0·993	0·941
9	0·45	0·800	0·975	0·961	0·45	0·794	0·987	0·941
10	0·50	0·800	0·987	0·941	0·50	0·794	0·987	0·941
11	0·55	0·800	0·984	0·961	0·55	0·794	0·987	0·941
12	0·60	0·806	0·968	0·992	0·60	0·807	0·987	0·941
13	0·65	0·813	0·944	0·997	0·65	0·834	0·980	0·932
14	0·70	0·813	0·926	0·949	0·70	0·862	0·987	0·936
15	0·75	0·820	0·919	0·905	0·75	0·896	0·987	0·941
16	0·80	0·862	0·906	0·876	0·80	0·931	0·993	0·961
17	0·85	0·924	0·902	0·863	0·85	0·965	0·993	0·982
18	0·90	1·000	0·944	0·880	0·90	0·978	1·000	0·997
19	0·95	0·993	1·007	0·979	0·95	0·993	1·000	1·000

Note: for the CCCC plate of 600 × 300 mm, $f_{0_1} = 136{\cdot}3$ Hz; $f_{0_2} = 152{\cdot}3$ Hz; $f_{0_3} = 219{\cdot}0$ Hz.

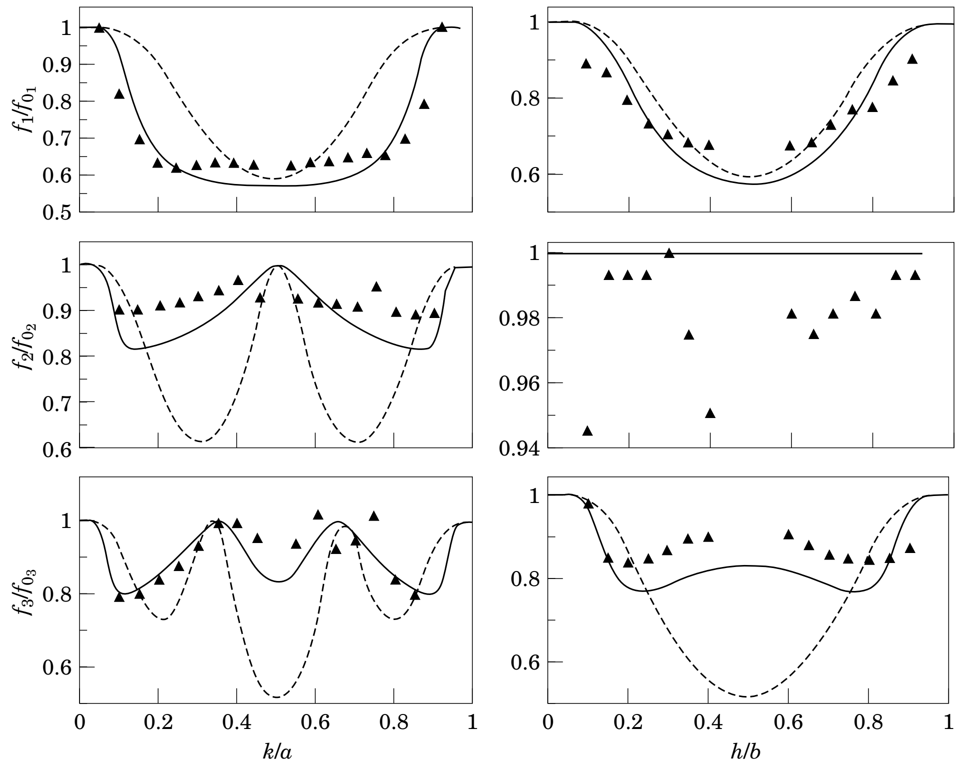

Figure 6. Comparative results of the 600 × 300 mm CCCC plate carrying a mass of 0.301 kg.

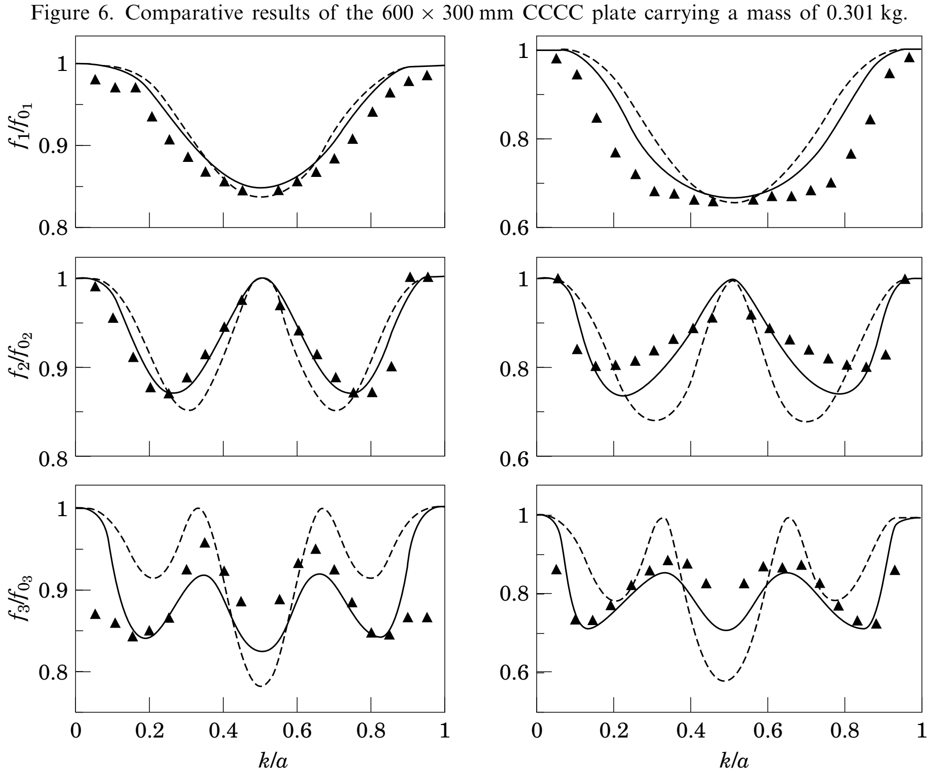

Figure 7. Comparative results of the 500 × 500 mm CCCC loaded plate. Key as Figure 5. Left-hand column mass = 0·096 kg; right-hand column mass = 0·301 kg.

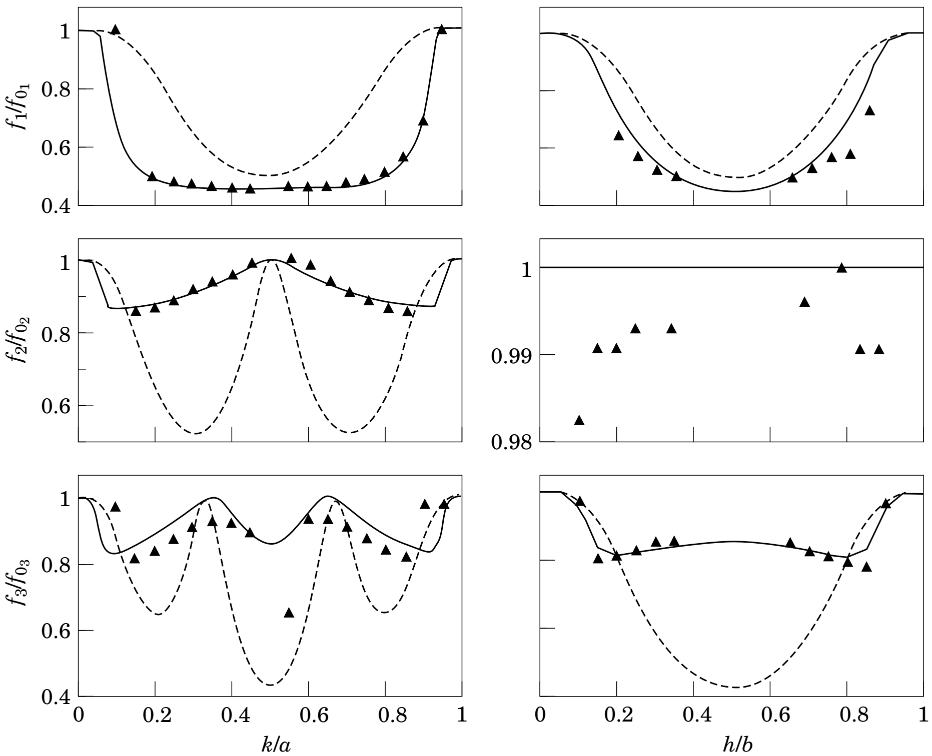

Figure 8. Comparative results of the 500 × 200 mm CCCC plate carrying a mass of 0·301 kg. Key as Figure 5.

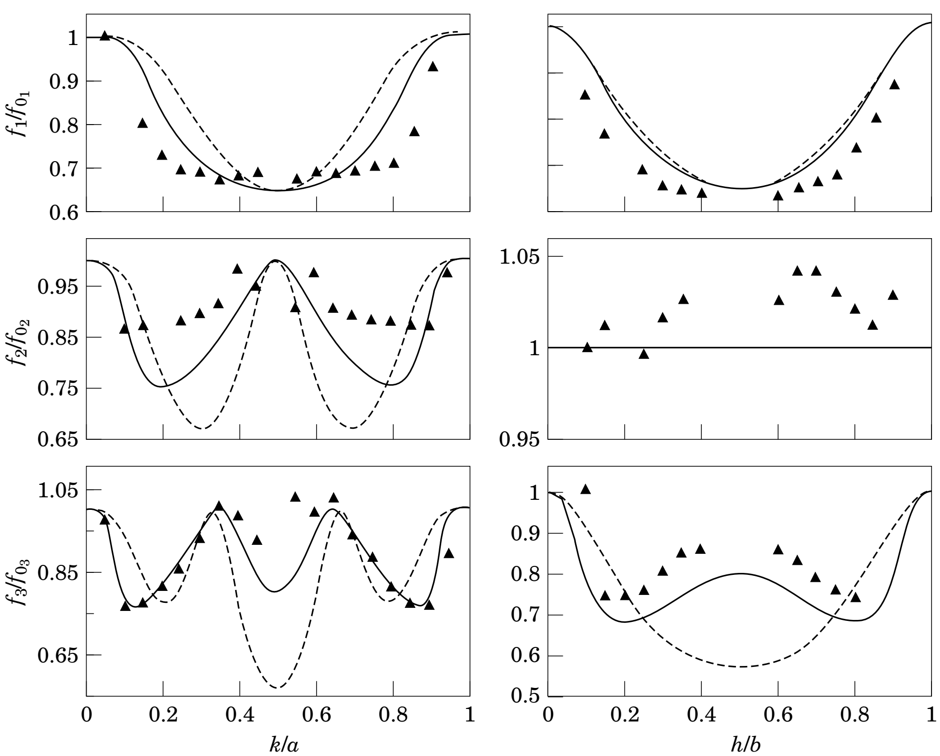

Figure 9. Comparative results of the 600 × 300 mm CSCS plate carrying a mass of 0·301 kg. Key as Figure 5.

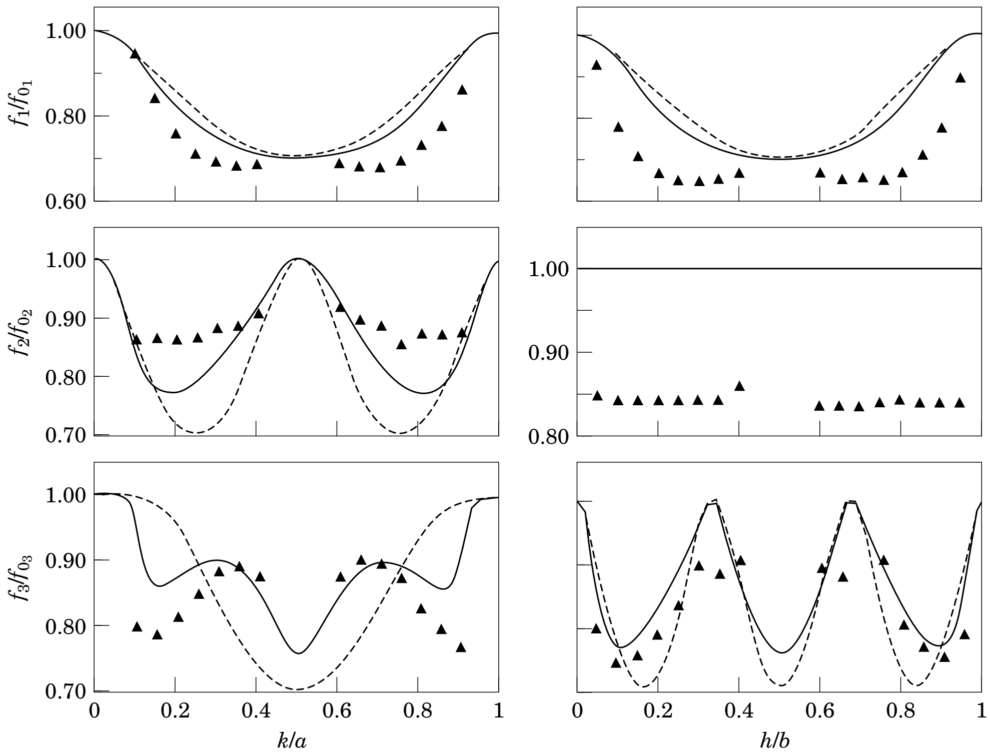

Figure 10. Comparative results of the 500 × 500 mm CSCS plate carrying a mass of 0·301 kg. Key as Figure 5.

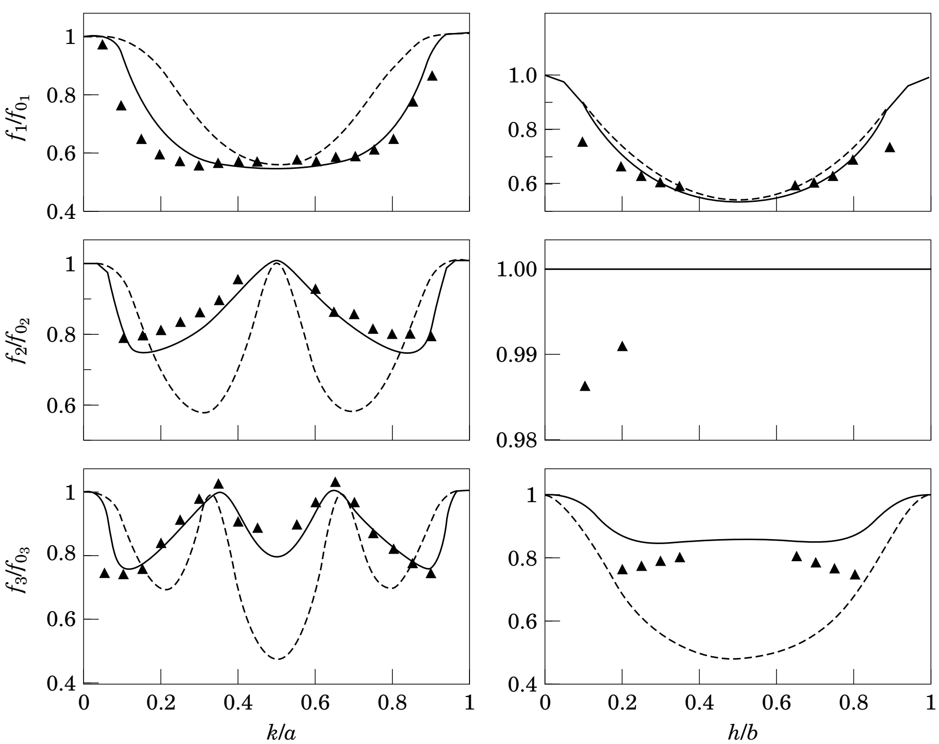

Figure 11. Comparative results of the 500 × 200 mm CSCS plate carrying a mass of 0·301 kg. Key as Figure 5.

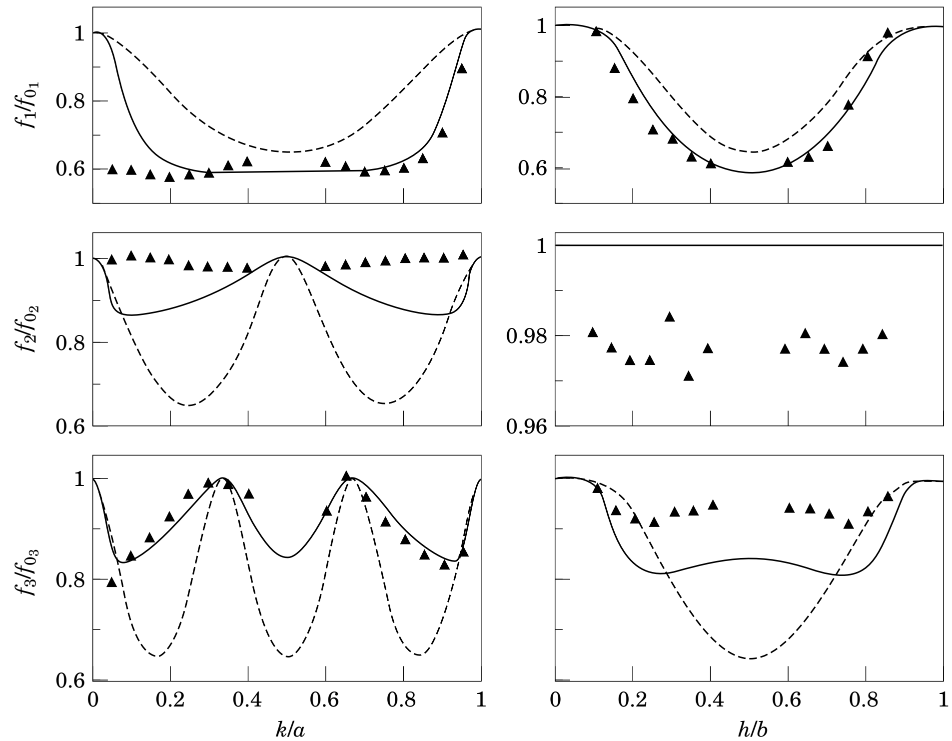

Figure 12. Comparative results of the 600 × 300 mm SCSC plate carrying a mass of 0·301 kg. Key as Figure 5.

amplifier. The real-time responses of the vibrating plate are plotted from which the resonance frequencies can be determined.

3. RESULTS AND DISCUSSIONS

3.1. FREQUENCY RATIOS FOR VARIOUS MASS LOCATIONS

Experimental testing was conducted by placing a concentrated mass at a grid point designated along the plate's centre-line on the x- or y-axis. The first three frequencies were

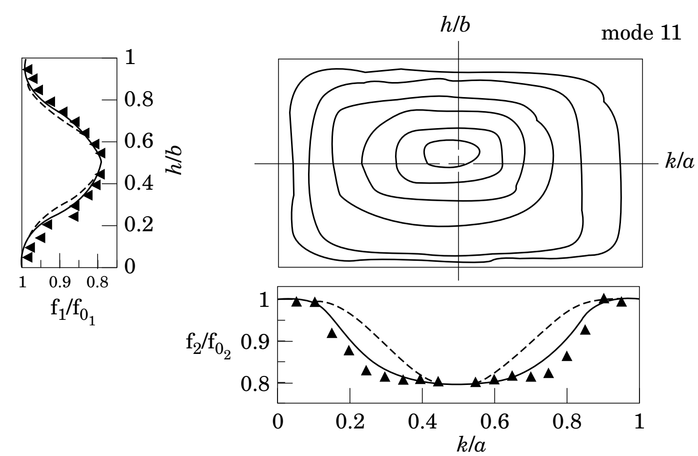

Figure 13. Sketch of the first mode shape for the 600 × 300 mm CCCC plate carrying a mass of 0·096 kg.

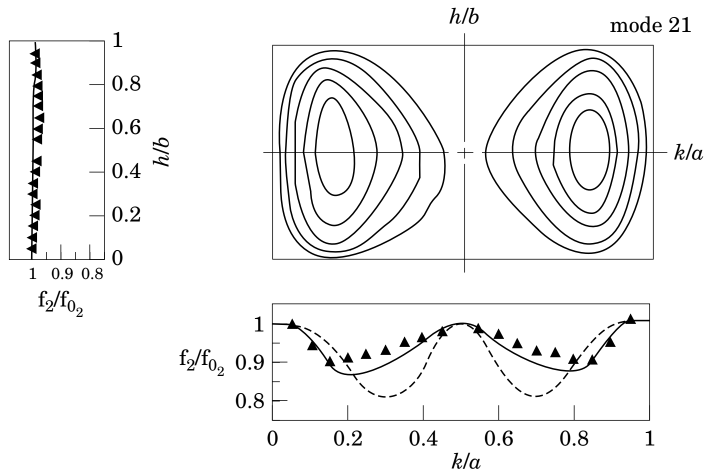

Figure 14. Sketch of the second mode shape for the 600 × 300 mm CCCC plate carrying a mass of 0·096 kg.

obtained and the experimental results were compared with the theoretical results from the EM one-term and 100-term models. It should be noted that the shaker of negligible mass was mounted at the plate's centre for all the experimental results presented here.

To show the change of the plate frequencies in a nondimensional form, the frequency ratio (f_n/f_{0n}) is plotted against the length ratio (k/a or h/b), as seen in Figure 5. Note that f_n is the frequency of mode n for the loaded plate, while f_{0n} is the frequency of mode n for the unloaded plate. For illustration, the experimental results for the 600 × 300 mm plate under the CCCC condition are presented in Table 3.

Results of different a/b ratios of the loaded plates under the CCCC boundary condition are shown in Figures 5–9, while those plates under the CSCS (short edges clamped, long edges simply-supported) conditions are shown in Figures 10 and 11. For the SCSC (short edges simply-supported, long edges clamped) condition, only results of the 600 × 300 mm plate are shown (see Figure 12). It is found that the EM 100-term model can generally predict accurately the experimental frequencies of the plates regardless of the position of concentrated mass, whereas the EM one-term model is only good for estimating the

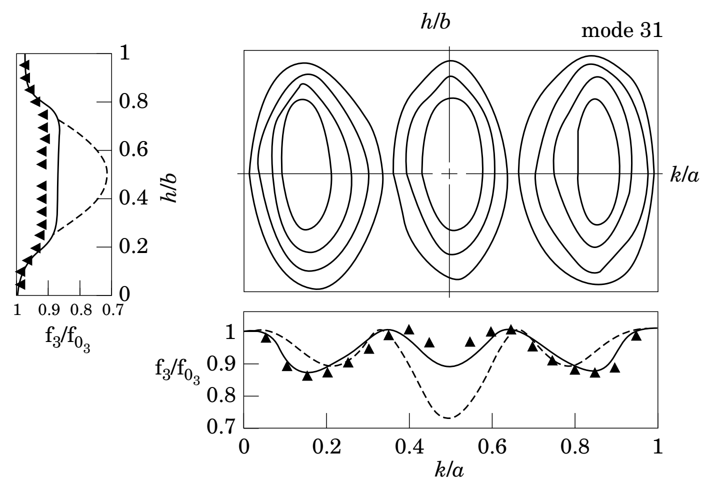

Figure 15. Sketch of the third mode shape for the 600 × 300 mm CCCC plate carrying a mass of 0·096 kg.

first-mode frequency of the plates carrying a centrally-placed mass. It is also found that the frequency curves of the loaded plates show similar trends when carrying different masses of 0·096 or 0·301 kg.

It is obvious that the h/b-direction for the 600 × 300 mm and 500 × 200 mm plates contain fewer nodes than that of the k/a-direction. This is expected as the plate's width ($b = 300$ or 200 mm) is smaller than its length ($a = 600$ or 300 mm).

3.2. PREDICTING MODE SHAPES USING ISO-FREQUENCY LINES

The mode shape of the plate at a particular frequency can be roughly sketched out by cross-referring the graphs of frequency-ratio versus length ratios of two directions, k/a and h/b. It should be mentioned here that the data presented for the mass locations along the two centre-lines is not sufficient for plotting contour lines of constant frequency ratios. For an accurate contour map of the iso-frequency ratios, one would really need to use a completed two-dimensional grid of the mass locations. The contour lines of constant frequency ratios for the first three natural frequencies presented here are extracted from the existing set of data coupled with the authors' intuition and previous experience on the subject [16, 17].

As an illustration, the curves shown in Figure 5 are used for this purpose. The frequency ratio curves for the first mode frequency shown in Figure 5 along the length and the width of the plate are sketched out in three dimensions. Contour lines of constant frequency ratios at various position aong the length and width of the plate are thus reproduced as shown in Figure 13. As it can be seen from the Figure, these contours are essentially similar to the fundamental mode shape of the plate. The other two higher modes results of Figure 5 are reproduced for the higher frequency mode shapes as shown in Figures 14 and 15. The contour lines of Figure 14 suggest that the plate is vibrating at mode 21, of the second natural frequency, while those of Figure 15 imply mode 31, of the third natural frequency. It has been demonstrated that one can easily relate an iso-frequency curve with the associated mode shape by virtue of the contour mapping method just demonstrated. This technique, as far as the authors know, has not been reported or published elsewhere.

4. CONCLUDING REMARKS

A vibration analysis of rectangular plates carrying a single mass along the plate's x- and y-centre-lines was carried out. Two opposite edges of the plate can either be both clamped or a combination of clamped and simply supported. The effects of added masses and their locations on the first three natural frequencies are of main concern. A shaker system was employed to obtain experimental frequencies, while an energy method was adopted in the numerical evaluation. It has been found that the EM 100-term model can generally predict well the experimental frequencies of singly loaded plates regardless of concentrated mass' position, whereas the EM one-term model is only good for estimating the first-mode frequency of singly-loaded plates with a centrally placed concentrated mass.

ACKNOWLEDGMENT

The authors wish to express their utmost gratitude to the reviewers for their valuable and constructive comments which have helped to improve the quality of the manuscript.

REFERENCES

1. W. F. STOKEY and C. F. ZOROWSKI 1959 *Transactions of the ASME*, *Journal of Applied Mechanics* **26**, 210–216. Normal vibrations of a uniform plate carrying any number of finite masses.
2. Y. C. DAS and D. R. NAVARATNA 1963 *Transactions of the ASME*, *Journal of Applied Mechanics* **30**, 31–36. Vibrations of a rectangular plate with concentrated mass, spring, and dashpot.
3. E. B. MAGRAB 1968 *Transactions of the ASME*, *Journal of Applied Mechanics* **35**, 411–412. Vibration of a rectangular plate carrying a concentrated mass.
4. P. A. A. LAURA, C. P. FILIPICH and V. H. CORTINEZ 1987 *Journal of Sound and Vibration* **117**, 459–465. Vibrations of beams and plates carrying concentrated masses.
5. K. H. LOW 1993 *Journal of Sound and Vibration* **168**, 123–139. An equivalent-center-weight factor method for predicting fundamental frequencies of plates carrying multiple masses from experimental test data.
6. K. H. LOW, G. B. CHAI and C. K. NG 1993 *Transactions of the ASME*, *Journal of Vibrations and Acoustics* **115**, 391–396. Experimental and analytical study of frequencies of an SCSC plate carrying a concentrated mass.
7. G. B. CHAI 1995 *Journal of Sound and Vibration* **179**, 170–177. Frequency analysis of a SCSC plate carrying a concentrated mass.
8. G. B. CHAI 1995 *Computers and Structures* **56**, 39–48. Frequency analysis of rectangular isotropic plates carrying a concentrated mass.
9. A. W. LEISSA 1973 *Journal of Sound and Vibration* **31**, 257–293. The free vibration of rectangular plates.
10. R. B. BHAT 1985 *Journal of Sound and Vibration* **102**, 493–499. Natural frequencies of rectangular plates using characteristic orthogonal polynomials in the Rayleigh-Ritz method.
11. R. B. BHAT, J. SINGH and G. MUNDKUR 1993 *Transactions of the ASME*, *Journal of Vibration and Acoustics* **115**, 177–181. Plate characteristic functions and natural frequncies of vibration of plates by iterative reduction of partial differential equation.
12. R. SZILARD 1974 *Theory and Analysis of Plates*: *Classical and Numerical Methods*. Englewood Cliffs, New Jersey: Prentice-Hall.
13. D. YOUNG 1950 *Transactions of the ASME*, *Journal of Applied Mechanics* **17**, 448–453. Vibration of rectangular plates by the Ritz method.
14. J. N. REDDY 1984 *Energy and Variational Methods in Applied Mechanics*. New York: John Wiley.
15. G. R. LINFIELD and J. E. T. PENNY 1989 *Microcomputers in Numerical Analysis*. Chichester: Ellis Horwood.
16. K. H. LOW 1993 *Journal of Sound and Vibration* **160**, 111–121. Analytical and experimental investigation on a vibrating rectangular plate with mounted weights.
17. K. H. LOW, C. K. NG and Y. K. ONG 1993 *ASCE Journal of Engineering Mechanics* **119**, 917–937. Comparative study of frequencies for plates carrying mass.